Steven Salah-Eddine
Andy Huu Huynh
Skyler Selvin
Yichi Ma

Light Scattering Meta-material

ME 303: Soft Composite & Soft Robotics

December 7, 2022

Abstract

Meta-materials with periodic patterns exhibit mechanical properties not found in nature. Their unique properties often find applications in impact mitigation and light scattering modulation, as demonstrated here. Inspiration is drawn from Yang and Ma's work [6], and the design is modified and scaled-up. FEA simulation of the proposed design shows near perfect contact when compressed to 0.75 strain, using FormLabs 50A elastomer as material with shear modulus 0.56 MPa. Simulated stress-stress curves for a single unit cell also show bi-stability and local buckling. The meta-material is 3D printed using Formlabs Elastic 50A Resin for high elasticity and compressibility and then compression tested. Dimensions of the compressed meta-material are measured to find respective lateral and longitudinal strains to yield a near-zero Poisson's ratio of 0.12. Binary ImageJ image of the compressed model shows only 7.6% light transmission, which is key for spatial control over the intensity of passing light. Stress-strain curves show a stable configuration at 0 strain. Fluctuating slopes of the stress-strain curve or elasticity suggests local buckling. Cyclic tests show repeatability and high hysteresis, indicating high energy dissipation properties for impact mitigation applications.

Introduction

Meta-materials are engineered materials usually with periodic patterns, showing properties not found in nature. They are made from assemblies of smaller unit cells, usually metals or plastics, and are arranged in repeating patterns, whose precise shape, geometry, size, and orientation affect the materials' smart properties. As a result, they have high strength, high deformability, high ductility, large elastic limit, low density, and high strength-to-weight ratio, which make them attractive candidates in the design of impact mitigation, shock-absorbing, and tunable materials. Shown in Fig. 1 is an example of a meta-material structure.

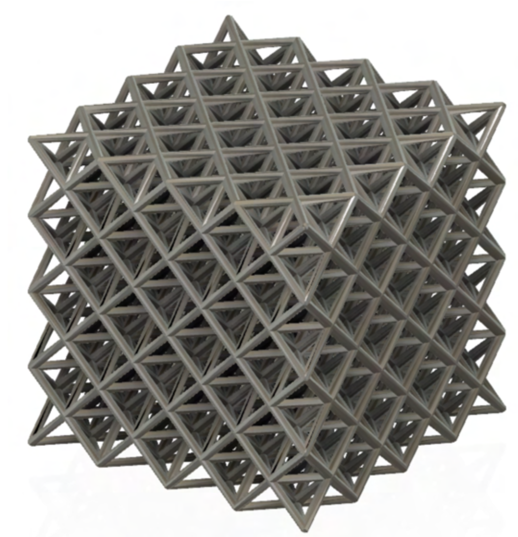

Figure 1: Octet meta-material structure

Recently, periodic patterned meta-materials with snap-through buckling have been shown to achieve significant elastic morphological change by switching or snapping between stable configurations [1]. These multi-stable meta-materials are often designed with shape-reconfiguration properties and zero Poisson's ratio [2,3,4]. While they usually find applications in deployable space structures, biomedical devices, and flexible electronics, these meta-materials can be used to control the propagation of scattered light as they compress and stretch. Such light scattering modulation is the basis of optical components such as diffraction gratings, Fresnel zone plates, and amplitude holograms [5].

In this work, a bi-stable mechanical meta-material with opposite or parallel snapping curved segments and zero Poisson's ratio is designed, 3D printed, and characterized. The meta-material is tested for impact mitigation and shock-absorbing potential as well as spatial control over the intensity of passing light.

Experimental Methods

The present meta-material design draws inspiration from Yang and Ma's work [6]. It contains opposite or parallel snapping curved segments with an elastic snap-through instability mechanism. A snapshot of the model is shown in Fig. 2. Buckling was exploited for obtaining mechanical bi-stability and energy dissipation effect, though the deformation remains well under the plastic threshold to ensure re-usability. Under pressure, unit cells having warped beam hairpin shape as shown initially experience high stiffness, bends upward/downward, and then stiffens again in the transition elastic zone, demonstrating bi-stability when the pin is upward/downward U-shaped and snap-through instabilities elsewhere. The present design modifies the pin thickness and scaling of the meta-material to have perfect contact when compressed and ease manufacturing.

Figure 2: Snapshot of meta-material with optical scattering modulation

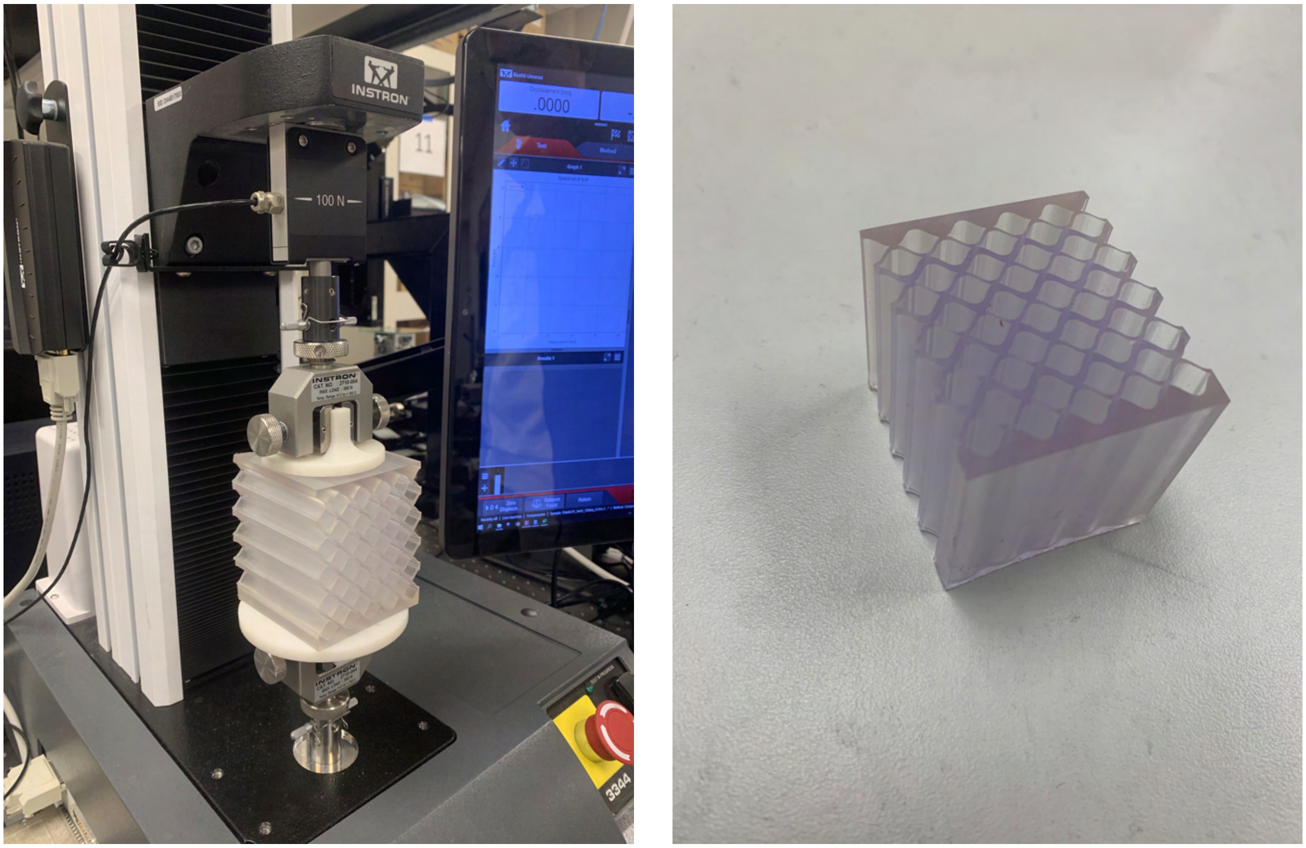

(a) (b)

Figure 3: a) Experimental setup on an Instron Universal Testing Machine, b) Fabricated meta-material sample using Resin 50A on FormLab SLA 3D Printer.

To ensure minimal air gaps between the unit cells when compressed, the deformation of the model was simulated in COMSOL with the nonlinear structural mechanics module (see fig. 4). Using a stationary study, a single unit cell was simulated consisting of two elastic beams. A set displacement as inflicted on one of two rigid domains attached to the elastic beams to study the behavior in compression. The periodicity of the unit cell was approximated with a 'symmetry' boundary condition for the lateral constraint on the unit cell. We also investigated a 'free' boundary conditions as well.

The model was 3D printed using Formlabs Form 3 SLA 3D printer with 25 µm resolution and 100um layer thickness. Formlabs Elastic 50A Resin was chosen for its high elasticity, ensuring repeated cycles without tearing under large deformation. Once printed, the model was rinsed with isopropyl alcohol (IPA 70) and cured for 30 minutes. Initial attempts at 3D printing such a thin design yielded torn unit cells, so the model was then scaled up. The finished product measures 75x75x84.5mm and is shown in Fig. 3.

To characterize its energy dissipation optical scattering properties, the meta-material was compression-tested using the Instron universal testing machine with a 100N load frame and software interface. Two plates were added above and below the meta-material for the even distribution of force during compression. In the simple loading-unloading test, the meta-material was compressed by 48mm (0.57 strain) at a strain rate of $0.01s^{-1}$. For the cyclic test, the material was first compressed by 24mm for 2 cycles than by 48mm for another 2 cycles.

Finite Element Analysis (FEA) Simulation

A single unit cell was simulated using COMSOL multi-physics. The simulation domain approximates the behavior of a single unit cell in the meta-material and derives the stress-strain relation for the unit cell which may be extended to an entire meta-material array of unit cells.

A two-dimensional simulation using the plane-strain approximation was chosen for simplicity and computational facility. Given that our structure is much deeper (15mm deep for the unit cell, 75mm deep for the entire meta-material array) than the beams of each unit cell are thin ($<$ 3mm), this approximation should be valid (plane-strain is valid for materials that are very thick in the direction of the plane of simulation, the z direction in our case). Linear discretization was used between mesh points, as this was found to have better convergence in the nonlinear solver.

To simulate the contact between the two elastomer beams, as well as the contact between the thinner bottom beam and the fixed rigid domain, I implemented contact pairs in COMSOL. Two contact pairs were simulated: between the two beams and between the lower beam and the bottom rigid domain. The contact between the upper rigid domain and the lower rigid domain may also come into contact, but empirically we can see that in the simulation it does not because the upper beam is stiffer than the lower.

The material Form 50A elastomer was modeled using the Neo-Hookean model $s = G(\lambda - \lambda^{-2})$, where s is the engineering strain and G is the shear modulus. The shear modulus was derived from the manufacturer's material data sheet. The cured Form 50A is reported to have a Shore A hardness of 50. Using the following formula in Ref. [7], we find the shear modulus of the material

$$G \approx \frac{\exp{(50 * 0.0235 - 0.6403)}}{3} \approx 0.56MPa$$

The model consists of a single unit cell elastomer, with rigid domains in the form of the neighboring unit cells on the top and bottom (see Fig. 4(b)). For the periodicity in the horizontal direction, a 'symmetry' boundary condition was used on the left and right of the unit cell. This boundary condition restricts the normal component of the displacement at the boundary to be zero with $\mathbf{u} \cdot \mathbf{n} = 0$, essentially making it a roller. Although the meta-material as an array can be expected to have some Poisson's ratio and will expand in the transverse direction somewhat, this effect will be small and the Poisson's ratio can be approximated as $\rho_{MM} \approx 0$, and the symmetry boundary condition should be a reasonable approximation. To simulate the effect of this approximation, we also conducted a simulation with free boundary conditions at the left and right edges of the unit cell.

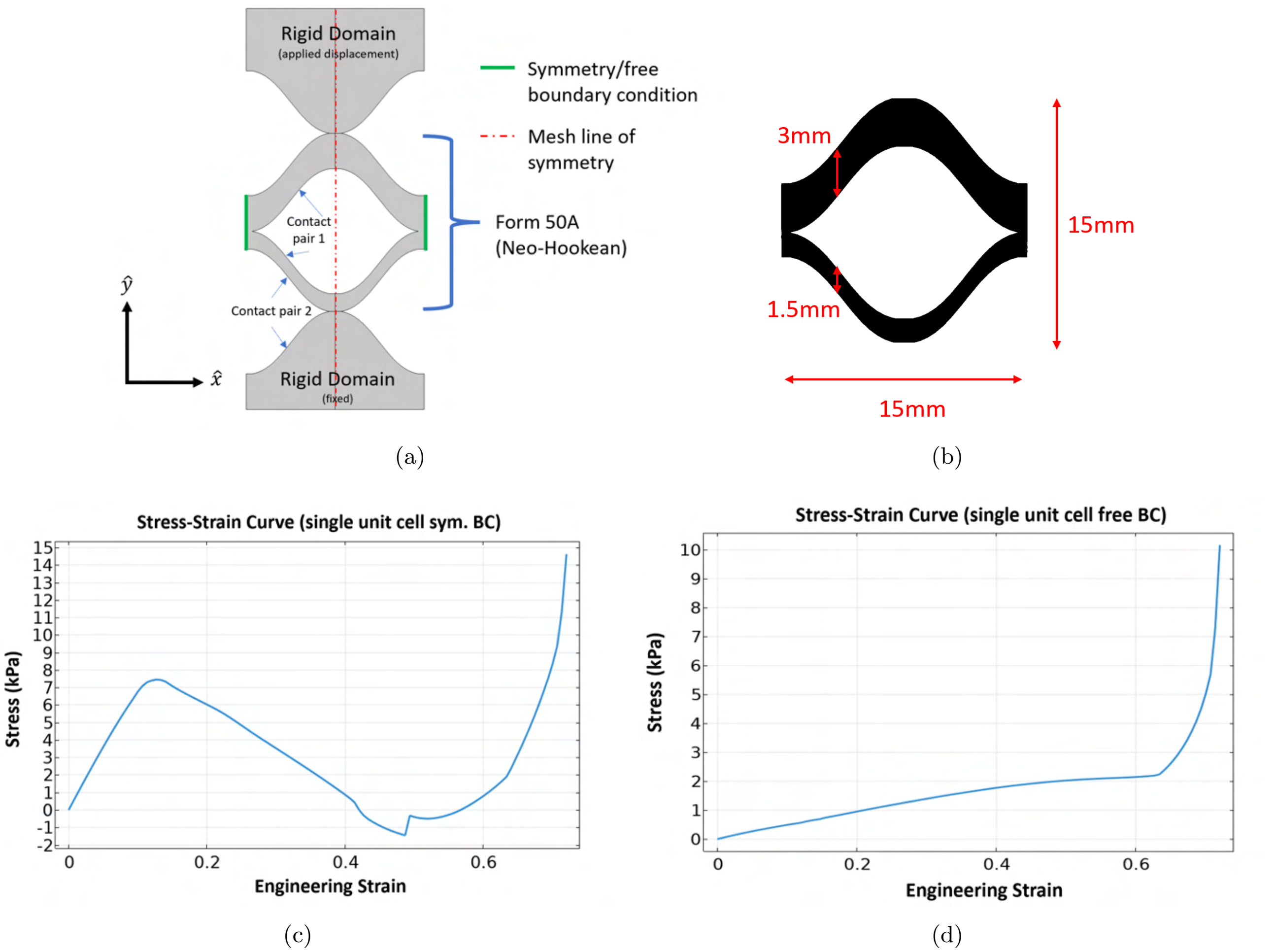

Figure 4: a) FEA simulation domain in COMSOL, b) Unit-cell diagram and dimensions, c) Stress-strain curve of a single unit cell with symmetry boundary conditions, d) Stress-strain curve of a single unit cell with free boundary. Compressive stress is shown as positive.

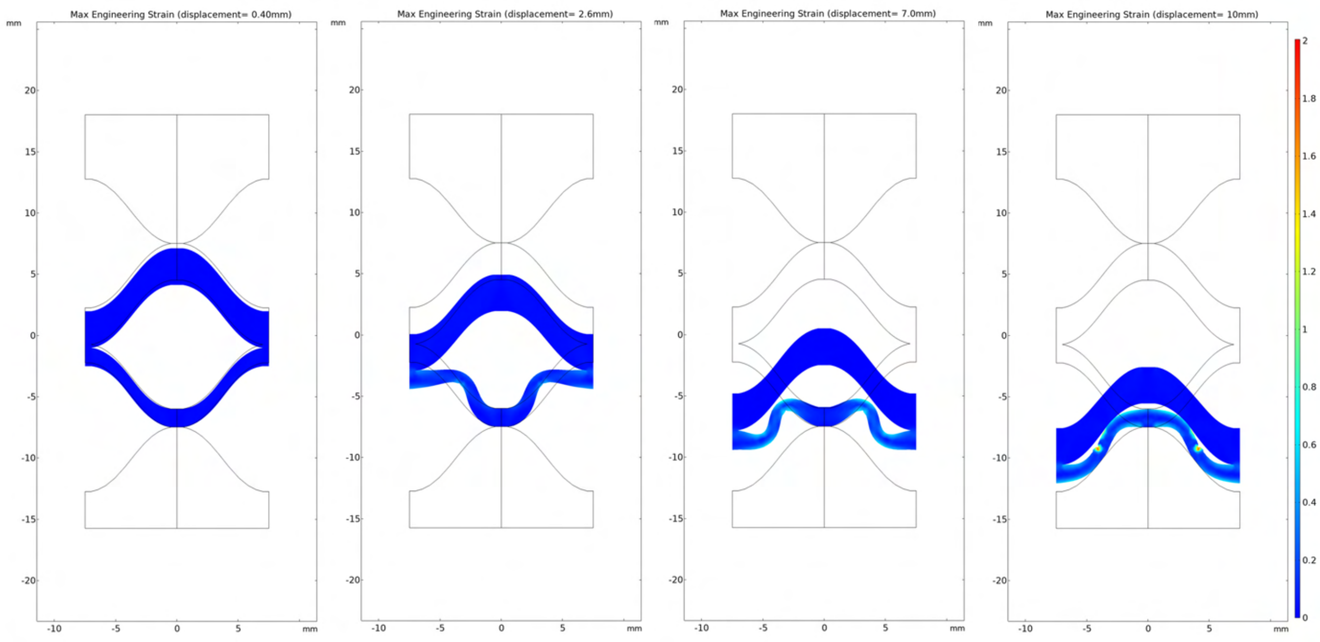

Figure 5: Engineering strain at different levels of compression for symmetry boundary conditions.

To simulate compression, a stationary study was conducted where the upper rigid domain was set to move in the $-\hat{y}$ direction $u_y \in [0, -10.8]$mm in 0.1mm steps, and remain fixed in the horizontal direction $u_x = 0$. The bottom rigid domain remained fixed in both directions. To ease the nonlinear solver, each subsequent 0.1mm simulation was initiated based on the previous step's solution. Thus, the changes in field solutions from solution to solution will be quasi-continuous and the solver will be less likely to fall into local minima.

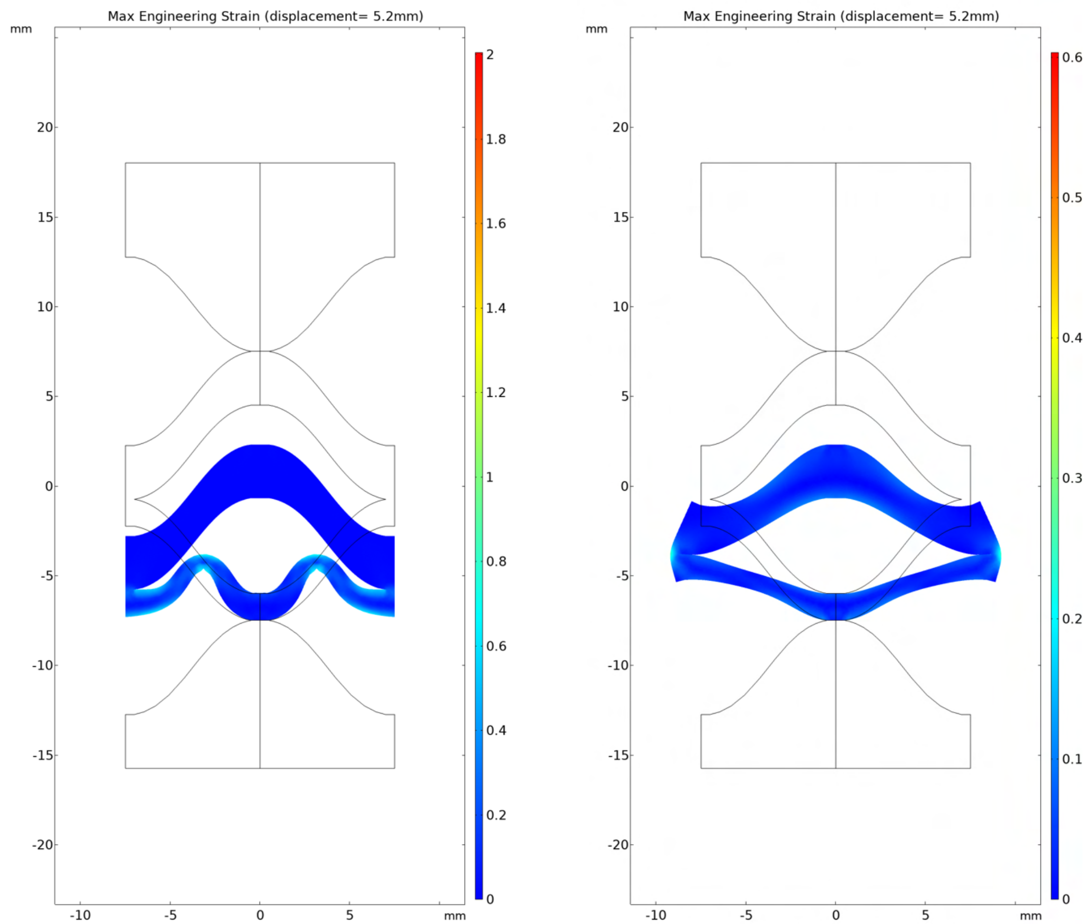

(a) (b)

Figure 6: a) Engineering strain at 5.2mm of compression for unit cell with symmetry boundary conditions, b) Engineering strain at 5.2mm of compression for unit cell with free boundary conditions

FEA Discussion

A stress-strain curve is derived from the simulation and shown in Fig. 4(c). At approximately 0.75 strain, the stress approaches infinity, indicating no further deformation with added pressure and therefore reaching full compression. This determination of maximum strain proves to be useful in later experimental tests. In addition, the elastic Young's modulus from a linear fit of the initial upward slope is calculated to be approximately 70 kPa. Beyond the critical point, the curve slopes downward, and the meta-material buckles at around 0.5 strain. Negative stiffness in this region can be thought of as instability and snapping from one stable state to another, as suggested. Thus, from the FEA simulation, the meta-material's abilities to fully compress and locally buckle, a desirable mechanism for energy dissipation, are demonstrated.

We can see from the stress-strain curve that stress actually falls below zero at around a strain of 0.4. Further, there are discontinuities here. The negative stress shows the truly bi-stable behavior of the meta-material, and the discontinuities capture the origin of this bi-stability: the buckling of the thinner lower beam. See the heat map of the strain during compression for details in Fig. 6. Here we can see a buckling of the lower beam, and snapping of it into a different conformation with different stress-strain behavior, thus causing a discontinuity of the stress-strain curve for the overall unit cell.

Under pressure, the upper thicker beam member hardly deforms, but the lower thinner member transitions from one stable U-shape mode to another. Visualization of its spatial deformation as a function of displacement is shown in Fig. 5.

The buckling behavior does not happen with free boundary conditions because we see a monotonically increasing stress-strain curve. Further, for the free boundary conditions, we see much less stress is required to deform the material, as it deforms in a way that reduces the isometric stress thus acting on the shear modulus instead of the bulk modulus.

When fully compressed so that the displacement is 10.8mm, the air gaps between the beams are not fully filled. Thus indicating that the optical scattering modulation may be limited. However, this happens because of the compliance of the top, thicker, beam and may not occur in the unit cell array. When simulating more than one unit cell stacked on top of each other, we found that for a three-unit cell stack, the middle unit cell's beams fully contact each other. For the purpose of this report on mechanical properties, the beam's full contact is not important and this discussion is not included here.

Experimental Results and Discussion

Once fabricated, the meta-material was compression-tested using the Instron universal testing machine. To verify near-zero Poisson's ratio, a snapshot of the fully compressed meta-material was post-processed in ImageJ using the uncompressed dimensions as the reference. The lateral and longitudinal strains were determined to be 0.0652 and 0.5341, respectively. Consequently, Poisson's ratio was calculated to be 0.1221, which is near-zero. Further, the amount of air gap allowing passing light was also determined in ImageJ by converting an image to binary color and measuring the relative shaded region. The process is shown in Fig. 7(b). As shown, when compressed to 0.57 strain, the meta-material traps 92.4% light, thus demonstrating light scattering property.

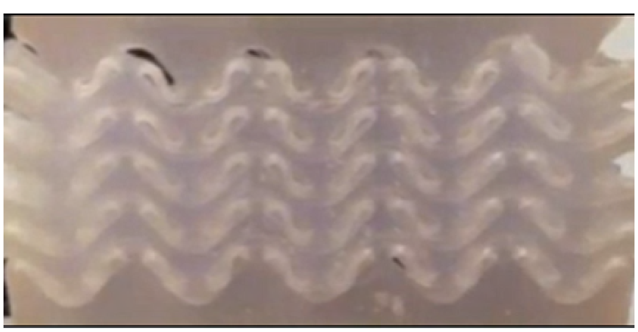

(a)

(b)

Figure 7: Conversion of an image of the compressed metamaterial to binary color for air gap measurements

The mechanical behavior of the meta-material is also investigated from the stress-strain data. In the loading behavior, there are six local minima on the stress-strain curve. This is reasonable since there are six layers of substructures. Meanwhile, the layers of the substructure have equal height, explaining that the local minimum occurs at the strain of 0.1, 0.2, 0.3, 0.4, and 0.5, as seen in Fig. 8(c). The structure only exhibits a single stable configuration at 0 strain since the potential energy increases monotonically with increasing strain. This allows the material to undergo huge deformation and return to its initial stage once the load is removed. The collapsing of the layers of the substructure limits the growth of the curve, allowing the material to be compressed further without applying too much stress.

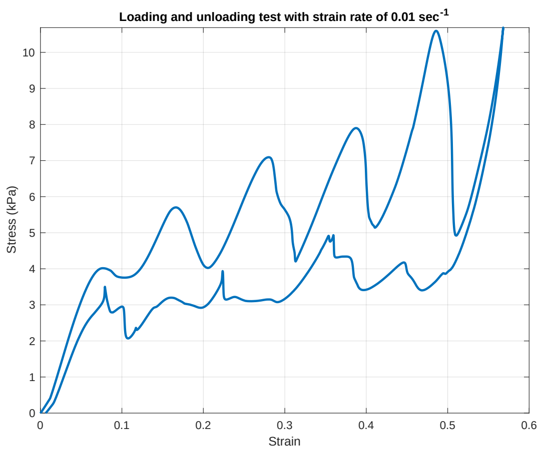

(a)

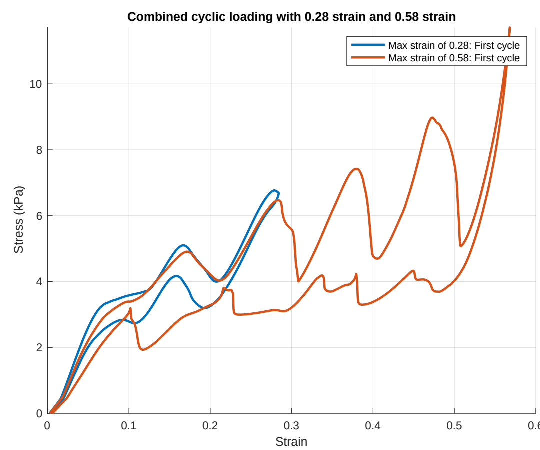

(b)

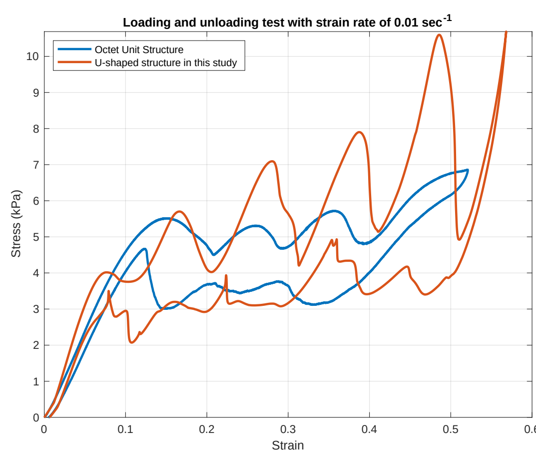

(c)

Figure 8: a) Simple loading and unloading compression test with max strain of 0.58 and strain rate of $0.01s^{-1}$, b) Comparison of the first cycle of 0.28 max strain test and 0.58 max strain test

As shown in Fig. 8(c), the unloading behavior forms a hysteresis, implying that the energy is dissipated through the loading and unloading test. The return curve is messier than the loading curve due to the uneven reverse snapping actions of each layer. According to the observation, some local reverse-snapping actions occurred at different layers. This means that snapping actions can happen at different locations of different layers. Such unorganized snapping actions in the unloading behavior result in “double peaks” and “sharp peaks” in the graph.

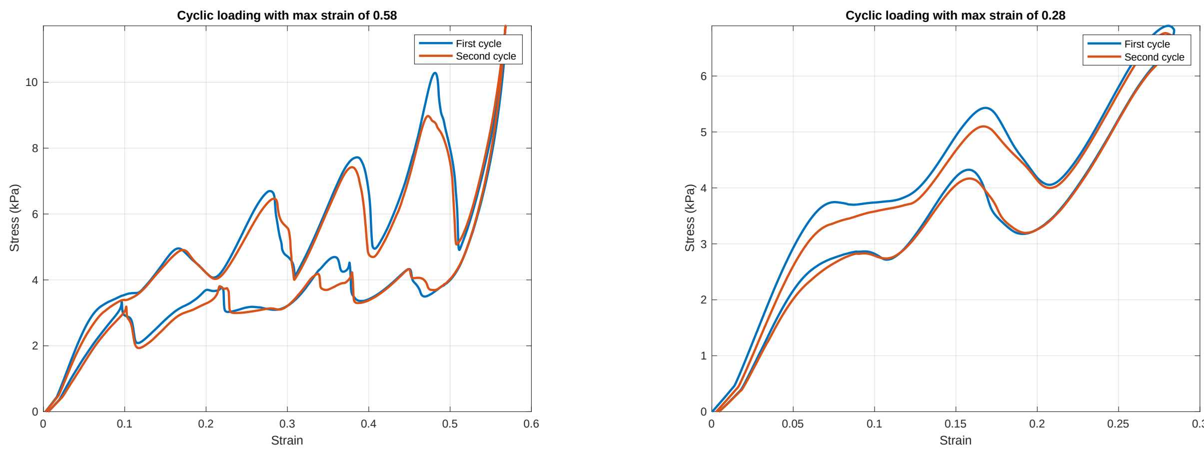

Figure 9: a) Cyclic loading with a max strain of 0.28 in two cycles, b) cyclic loading with a max strain of 0.28 in two cycles

The first cycles of the compression test to the max strain of 0.28 and max strain of 0.58 are plotted in Fig. 8(b) for comparison. In the 0.28 strain test, only two layers of the substructures snapped. Compared to the 0.58 strain test, six layers are fully collapsed. It is obvious that the unloading curve of the 0.28 strain test is more consistent than the unloading curve of the 0.58 strain test. This is because there are no messy reverse-snapping actions that occur when returning from a small strain. According to the observation, the layers of the structure unfold one by one.

The inconsistency of the unloading behavior is caused by the imperfection of the material. Some structure walls are thicker than others. The density of the material might not be evenly distributed. Such imperfection mainly resulted in fabrication or curing processes.

Conclusions

A metamaterial structure consisting of warped beam pin unit cells was designed, fabricated, and tested. Drawing inspiration from Yang and Ma’s previous work [6], the design has to snap curved segments with an elastic snap-through instability mechanism and is now repurposed for light scattering modulation and potential impact mitigation applications. The metamaterial was 3D printed with Formlabs Form 3 SLA 3D printer using Formlabs Elastic 50A Resin for high elasticity. FEA simulation showed complete closure of the unit cells at 0.75 strain, though the experiment only reached 0.57 strain. Nevertheless, the binary image of the compressed material showed trapping of 92.4% light at 0.57 strain. The compressed dimensions were also measured, and Poisson’s ratio was determined to be 0.1221, which is near zero. Experimental stress-strain curves showed local buckling, suggesting the potential for high energy dissipation for impact mitigation purposes.

References

[1] D. Restrepo, N.D. Mankame, and P.D. Zavattieri, "Phase transforming cellular materials," Extreme Mech Lett 4 (2015) 52-60.

[2] H. Yang and L. Ma, "Multi-stable mechanical metamaterials with shape-reconfiguration and zero Poisson's ratio," Mater Design 152 (2018) 181-190.

[3] A. Rafsanjani and D. Pasini, "Bistable auxetic mechanical metamaterials inspired by ancient geometric motifs," Extreme Mech 9 (2016) 291-296.

[4] T.A. Hewage et. al., "Double-negative mechanical metamaterials displaying simultaneous negative stiffness and negative Poisson's ratio properties," Adv Mater 28 (2016) 10323-10332.

[5] P. Cencillo-Abad, N.I. Zheludev, and E. Plum, "Metadevice for intensity modulation with sub-wavelength spatial resolution," Scientific Reports 6 (2016) 37109.

[6] H. Yang and L. Ma, "Multi-stable mechanical metamaterials by elastic buckling instability," J Mater Sci 54 (2019) 3509-3526.

[7] K. Larson, "Estimating Elastic Modulus from Durometer Hardness for Silicones," Dow Corning Corporation (2016).